Nitric Oxide 93 (2019) 44–52

Contents lists available at ScienceDirect

Nitric Oxide

journal homepage: www.elsevier.com/locate/yniox

Interleukin enhancement binding factor 3 inhibits cardiac hypertrophy by targeting asymmetric dimethylarginine-nitric oxide

Ruo-Han Yang[a,b,1], Xing Tan[b,1], Lian-Jie Ge[b,1], Jia-Cen Sun[b], Xiao-Dong Peng[a], Wei-Zhong Wang[b,*]

[a] Department of Pharmacology, College of Pharmacy, Ningxia Medical University, 1160 Shengli Street, Yinchuan, 750004, China
[b] Department of Physiology, Second Military Medical University, Shanghai, 200433, China

ARTICLE INFO

Keywords:
Cardiac hypertrophy
Angiotensin II
Interleukin enhancement binding factor 3
Nitric oxide
Asymmetric dimethylarginine

ABSTRACT

Persistent cardiac hypertrophy eventually leads to deterioration of heart function and changes to normal morphology. Decreased nitric oxide (NO) production plays a critical role in modulating cardiac hypertrophy. Interleukin enhancement binding factor 3 (ILF3), a member of the double-stranded RNA-binding protein family, is known to regulate the transcription and stability of mRNA. Therefore, the major aim of the present study was to determine the role of ILF3 in reduction of NO production in cardiac hypertrophy. Cardiac hypertrophy models of neonatal rat cardiomyocytes (NRCMs) and adult rats were induced by angiotensin II (Ang II) in this study. First, it was found that ILF3 expression, NO production, and nitric oxide synthase (NOS) activity was decreased in cultured cardiomyocytes and adult rats treated with Ang II, compared with NRCMs treated with vehicle and rats treated with saline infusion, respectively. These effects induced by Ang II were significantly exacerbated by specific ILF3 knockdown. Moreover, the level of asymmetric dimethylarginine (ADMA), an endogenous inhibitor of NOS, was increased significantly in the Ang II-induced hypertrophic NRCMs and adult rats. Additionally, decreased protein expression and mRNA level of dimethylarginine dimethylaminohydrolases 1 (DDAH1, which degrades ADMA) were observed. Furthermore, specific ILF3 knockdown further aggravated these effects, but didn't reduce the expression level of NOS isoforms. In conclusion, our data show that ADMA accumulation-mediated decrease in NO production plays an important role in cardiomyocyte remodeling, which may be associated with ILF3-mediated DDAH1 reduction.

1. Introduction

Cardiac hypertrophy is an adaptive remodeling of cardiomyocytes to adapt to the pathological changes induced by increased pressure loading, which is characterized by increased cardiomyocyte size [1,2]. However, the persistent pathological hypertrophy eventually leads to deterioration of heart function and morphology [3,4]. Numerous molecular mechanisms have been studied in the hypertrophic process, such as the mitogen-activated protein kinase (MAPK) signal transduction pathway [5], oxidative stress [6,7], nitric oxide synthase (NOS) abnormality [8], post-transcriptional modification of mRNA [9], inflammation [10], and free fatty acids [11], etc. However, the underlying mechanisms during the development of cardiac hypertrophy are rather complicated and have yet to be elucidated completely.

Nitric oxide (NO), a small gaseous molecule, is produced in every cell type in the heart [12]. It has been reported that NO donors L-arginine and endogenously formed NO through overexpression of endothelial nitric oxide synthase (eNOS) were shown to blunt the hypertrophic response to isoproterenol stimulation in cultured cardiac myocytes and mice [13,14]. Nonselective inhibition of NOS prevented exercise training-mediated up-regulation of phosphorylated endothelial NOS and plasma NO in isoproterenol-induced cardiac hypertrophic mice [15]. These findings suggest that NO exerts anti-hypertrophic properties in cardiomyocyte. However, the mechanism of abnormal NO production in cardiac hypertrophy is not clear. The endogenous inhibitor of NOS-asymmetric dimethylarginine (ADMA), mainly synthesized by protein arginine methyltransferase (PRMT) and degraded by dimethylarginine dimethylaminohydrolases (DDAH), is a strong predictor of adverse cardiovascular outcomes [16]. In hemodialysis patients, raised plasma concentration of ADMA is associated with concentric left ventricular hypertrophy and adverse cardiovascular outcomes in patients with end-stage left ventricular dysfunction [17].

* Corresponding author. Department of Physiology, Second Military Medical University, 800 Xiangyin Road, Shanghai, 200433, China.
E-mail address: wangwz68@hotmail.com (W.-Z. Wang).
[1] The authors contributed equal to this study.

https://doi.org/10.1016/j.niox.2019.09.002
Received 2 February 2019; Received in revised form 2 September 2019; Accepted 10 September 2019
Available online 17 September 2019
1089-8603/

But whether there is a causal relationship between ADMA and cardiac hypertrophy remains unclear.

Interleukin enhancement binding factor 3 (ILF3) is a member of the double-stranded RNA-binding protein encoded by the *ILF3* gene located on human chromosome 19 [18]. The main function of ILF3 protein is to regulate the transcription and stability of mRNA, and promote the transfer of mRNAs bound to the ILF3 protein from the nucleus to the cytoplasm, facilitating the translation process [19,20]. The A to G polymorphism (rs2569512) of *ILF3* was significantly associated with myocardial infarction in Japanese individuals by a genome-wide association study [21]. In addition, ILF3 stabilizes proangiogenic transcripts including vascular endothelial growth factor, chemokine (C-X-C motif) ligand 1, and interleukin-8 in cultured human coronary artery endothelial cells (hCAECs), suggesting that ILF3 plays a novel and critical role in angiogenesis [22]. However, it is not clear whether ILF3 can regulate the process of cardiac hypertrophy. Interestingly, it has been reported that there is an interaction between ILF3 and PRMT1 [23,24], which is involved in the regulation of NO production through accumulating ADMA [25]. It is not clear whether ILF3 affects NO production by regulating PRMT1 and ADMA, and thereby participate in the regulation of cardiac hypertrophy.

In the present study, we have observed that ILF3 expression is downregulated in hypertrophic cardiomyocyte induced by angiotensin II (Ang II) in both *in vivo* and *in vitro* experiments. Therefore, we aimed to determine: 1) the effect of ILF3 on the cardiac hypertrophy via inhibition of NO production; and 2) the underlying mechanisms by which ILF3 inhibits NO production by accumulating ADMA in cardiomyocytes.

2. Methods

2.1. Animals

One-day old Sprague Dawley (SD) neonatal rats and sixteen-week old male SD adult rats were purchased from Sino-British SIPPR/BK Laboratory Animal Ltd (Shanghai, China) and used in this study. Adult rats were kept in a 12/12-h light and dark animal room, and had free access to water and food. All experimental procedures were approved by the Institutional Animal Care and Use Committee of the Second Military Medical University, and all animal operations in this study were performed by following the Guide for the Care and Use of Laboratory Animals published by the US National Institutes of Health.

2.2. Rat cardiac hypertrophy model

According to a previous study [26], rats were treated with continuous infusion of Ang II ($0.7\ mg\ kg^{-1}\ d^{-1}$) by subcutaneously implanting an osmotic minipump (Alzet model 2ML4, DURECT Co). In brief, the osmotic minipumps were pre-loaded with saline (n = 15) or Ang II (n = 15) dissolved in sterile solution according to the manufacturer's instruction. Male SD rats (200–300g) were anaesthetized by inhaling 3% isofluorane, followed by removal of hair on the back. A 3–5 cm incision was made in the back of each rat, the subcutaneous tissue was bluntly separated, the osmotic pump was then implanted into the subcutaneous tissue space, and finally the skin was sutured. Four weeks after treatment, rat hearts were harvested, weighed, and rapid-frozen in liquid nitrogen.

2.3. Measurements of blood pressure (BP)

As described in our previous study [27], in brief, rats were anaesthetized by intraperitoneal injection of urethane (800 mg/kg) and α-chloralose (40 mg/kg). The trachea was cannulated. The right femoral artery was catheterized for measuring BP and heart rate (HR) through a Powerlab system. The body temperature was kept at 37 °C using a temperature controller. The right femoral vein was cannulated for maintaining anesthesia via supplementing α-chloralose (10 mg/kg).

2.4. Histological analyses

Four weeks after continuous infusion of Ang II or saline, the rats were euthanized with an overdose of pentobarbital sodium (200 mg/kg) to assess the status of hypertrophic growth. The hearts were collected and weighed for calculating the following ratio: heart mass/body mass (‰). Hearts of the rats were fixed in 4% paraformaldehyde and then sectioned transversely at 5 μm in the region close to the apex to visualize the left and right ventricles. Partial sections were stained with hematoxylin and eosin (H&E) to evaluate histopathologic changes in cardiomyocyte size. The sections were visualized by light microscopy. To verify the transfection efficiency of siRNA, sections were then mounted on slides after three 5 min washes and cover slipped with antifade medium. The FAM fluorescence was detected by a fluorescence microscope (Olympus).

2.5. Western blot analysis

Total proteins were extracted from the left ventricle tissues, kidney, liver, and brain of experimental rats and cultured neonatal rat cardiomyocytes (NRCMs), lysed, sonicated, and centrifuged. The protocols used for Western blot were described previously [28]. In brief, the protein samples were collected by extracting the supernatants. The protein concentrations of samples were then measured by a BCA kit. The protein samples were denatured with loading buffer and heated to 100 °C for 10 min. After denaturation, protein samples (30 μg) were loaded onto a 10% SDS–PAGE gel and then transferred to a PVDF membrane. The membrane was incubated with primary antibody [anti-ILF3 (no. ab50832, abcam); anti-PRMT1 (no. ab190892, abcam); anti-DDAH1 (no. ab180599, abcam); anti-DDAH2 (no. ab184166, abcam); anti-nNOS (no. 610308, BD Transduction labs); anti-eNOS (no. 9586, CST); and anti-iNOS (no. 13120, CST)] after blocking for 2 h with 5% milk dissolved in Tris-buffered saline tween (TBST) overnight at 4 °C. In order to detect primary antibodies, the membranes were washed 3 times with TBST and then incubated with peroxidase-conjugated secondary antibodies for 2 h at room temperature. The protein bands were visually detected with the chemiluminescent agent and analyzed by the GeneTools software (Gene Company). The expression level of target proteins was normalized to α-tubulin.

2.6. Quantitative real-time PCR

In order to detect cardiac hypertrophy from the molecular marker level, total mRNA extraction of left ventricle tissues and cultured NRCMs were performed by an EASYspin RNA Mini Kit (Aidlab Biotechnologies, Beijing, China) according to the manufacturer's instructions. Twenty μg extracted mRNA of all samples were used to synthesize cDNA via reverse transcriptase reaction using ReverTra Ace® qPCR RT Master Mix kit (Toyobo Co. LTD., Japan) according to the manufacturer's protocol. One μL cDNA template and 0.5 μL primers were added to 12.5 μL 2 × SYBR qPCR Mix (Aidlab Biotechnologies, Beijing, China). The conditions of cDNA amplification for ILF3, atrial natriuretic peptide (ANP), β-myosin heavy chain (β-MHC), and GAPDH gene were 94 °C for 3 min, denaturation at 94 °C for 10 s, followed by annealing and extension at 60 °C for 30 s. Subsequently, the target genes expressions were normalized to GAPDH gene expression. The primers for qPCR are shown as follows: ANP-rat: 5′-GACATGCCGCCTGGAGAAAC-3' (forward), 5′-AGCCCAGGATGCCCTTTAGT-3' (reverse). β-MHC-rat: 5′-GCAGCTTATCAGGAAGGAATAC-3' (forward), 5′-CTTGCGTACTCTGTCACTC-3' (reverse). ILF3-rat: 5′-AGCACGGCAAGAATCCTGTAATGG-3' (forward), 5′-TTCTGTCCGTCCACCTCAACCTC-3' (reverse). GAPDH-rat: 5′-GACATGCCGCCTGGAGAAAC-3' (forward), 5′-AGCCCAGGATGCCCTTTAGT-3' (reverse).

2.7. ELISA

The protein sample extraction method prepared for the ELISA is consistent with the protein extraction steps described in the Western blot. The experimental process of ELISA was based on our previous study [29]. Briefly, the supernatants were extracted after centrifugation, the protein concentration of each protein sample was measured using a BCA kit, and the levels of ADMA in left ventricle tissues of experimental rats and cultured NRCMs were detected via ELISA kits (Shanghai Westang Bio-tech Co., LTD) in accordance with the manufacturer's instructions. The levels of ADMA were determined at absorbance of 450 nm with an automated microplate reader. Finally, a standard curve was made, and the ADMA content of all samples were calculated based on the standard curve.

2.8. Total NO production detection

According to our previous study [29], the NO production in left ventricle tissues and cell culture medium of NRCMs were detected. The left ventricle tissues of different treated rats were lysed with cell and tissue lysis buffer (purchased from Beyotime Biotechnology, #S3090) specific for NO Assay. The supernatants were extracted after centrifugation, and the protein concentrations of all samples were determined via a BCA kit. Total NO production in the left ventricle tissues and in cell culture medium of NRCMs was determined by measuring the concentration of nitrate and nitrite through the Total Nitric Oxide Assay Kit (purchased from Beyotime Biotechnology, #S0023) in accordance with the manufacturer's instructions. The levels of nitrate and nitrite were determined at an absorbance of 540 nm with an automated microplate reader, and were calculated for each sample according to standard curve. The total amounts of NO in all samples were measured by the ratio of the nitrate and nitrite content to the corresponding sample protein concentration.

2.9. DDAH activity detection

DDAH activity was detected by the conversion of L-citrulline from ADMA, as described previously [30]. In brief, the homogenate of heart tissues (50 μl) was incubated with 1 mmol/L ADMA (ADMA in 0.1 mol/L phosphate buffer solution) for 30 min at 37 °C. 10% trichloroacetic acid was used to stop the reaction. The samples were centrifuged, and the supernatant was then incubated with diacetyl monoxime (0.8%) and antipyrine (0.5%) for 110 min at 60 °C. Spectrophotometric analysis was used to determine the amounts of L-citrulline formed at 466 nm. In order to obtain background value, the homogenate was subjected to the same determination process of DDAH activity in the absence of ADMA. DDAH activity was obtained by sample data subtracting the background value. One unit of the enzyme was defined as the amount that catalyzed the formation of 1 mmol/L L-citrulline from ADMA per minute at 37 °C.

2.10. Measurement of total NOS activity

The assay for total NOS activity measurement was carried out as previously described [30]. The concentration of total protein in the heart tissue and NRCMs was measured using the BCA kit. The NOS activity was assessed using a Total Nitric Oxide Synthase assay kit (Nanjing Jiancheng Biotechnology Institute, Nanjing, China). The assay was carried out according to the instructions provided by the manufacturer. Data were expressed as U/mg protein in heart tissue.

2.11. Primary cardiomyocyte culture

NRCMs were isolated from one-day-old SD rat hearts. According to a previous study [31], the entire heart of the newborn rats was excised, cut into small pieces, and digested with 0.25% mixed trypsin (BSA 40 mg, collagenase II 9–10 mg, DNase 2–3 mg, dissolved in 40 ml DMEM-high glucose medium). Primary cells were collected after passing through a 40 μm cell strainer, and then were seeded in tissue culture dishes. Fibroblasts were removed using a differential attachment technique. The supernatants that contained cardiomyocyte were collected and NRCMs were seeded onto six-well culture plates in DMEM-high glucose medium containing 20% fetal bovine serum and penicillin/streptomycin. Inhibition of fibroblast proliferation was performed by treating with BrdU. Subsequently, these cells were treated with Ang II (1 μmol/L), Ang II combined with Ang II type I receptor blocker (losartan, 10 μmol/L, Sigma Aldrich Co., St. Louis, MO, USA) or PBS for 48 h. The cardiomyocyte on glass cover slips were fixed with 4% paraformaldehyde for 20 min at room temperature to visualize the cardiomyocytes morphology by microscopy. The myocardial cell size was measured using Image Pro Plus software after treatment with Ang II and/or ILF3 knockdown.

2.12. In vivo ILF3 knockdown

After SD rats were established as a model of cardiac hypertrophy, these rats were further received direct intramyocardial injection of ILF3 or scramble small interfering RNA (siRNA) on the left ventricular wall with at three days before the sacrifice of the rats, in order to specifically inhibit cardiac ILF3 expression. According to a previous study [32], briefly, carboxyfluorescein (FAM)-labeled siRNAs were diluted in 5% glucose and mixed with *in vivo*-jet PEI (Polyplus-transfection, France). The *in vivo*-jet PEI system is a linear polyethylenimine, which mediates efficient siRNA delivery to a wide range of tissues. The protocol is as follows: the *in vivo*-jet PEI (0.36 μl reagent)/nucleic acid (30 μg nucleic acid) complexes were prepared in a laminar flow hood using sterile 10% glucose solution (100 μl). The complexes were incubated at room temperature for 15 min. Cardiac hypertrophy model rats were anaesthetized by inhaling 3% isofluorane again, and the heart was exposed via left thoracotomy at the fifth intercostal space. Twenty microliters of ILF3 specific or scramble siRNAs (dose 0.8 μg/ml) were injected directly into the left ventricular wall at 5 different sites with a 32G needle. Seventy-two hours after the siRNA injection, the rats were euthanized with an overdose of pentobarbital sodium (200 mg/kg) and their hearts were collected.

2.13. In vitro ILF3 knockdown

To knockdown ILF3 expression, rat ILF3 targeted siRNA were designed and synthesized by GenePharma (Shanghai). Non-targeting scramble siRNA was used as the control. Sequences of siRNAs were as follows: ILF3-rat: 5′-CCAGAUGGUUCUGGCAUUUTT-3' (forward), 5′-AAAUGCCAGAACCAUCUGGTT-3' (reverse). Scramble: 5′-UUCUCC GAACGUGUCACGUTT-3' (forward), 5′-ACGUGACACGUUCGGAGA ATT-3' (reverse). According to a previous study [33], the siRNAs were transfected into cells using Lipofectamine 2000 (Invitrogen, US) according to manufacturer's instructions. Interference efficacy was evaluated by fluorescence microscope and Western blot.

2.14. Data analysis

All data are expressed as mean ± SEM. BP is expressed by mean arterial pressure. Unpaired student's t-test was used for comparing the differences in BP, the ratio of heart mass to body mass, total NO production and the expression levels of ILF3 protein between SD rats treated with Ang II or saline. Above parameters of differences between SD rats and NRCMs stimulated with Ang II or saline combined with ILF3 or scramble siRNA were analyzed using the one-way ANOVA followed by Bonferroni's post hoc test. $P < 0.05$ was considered to be significant.

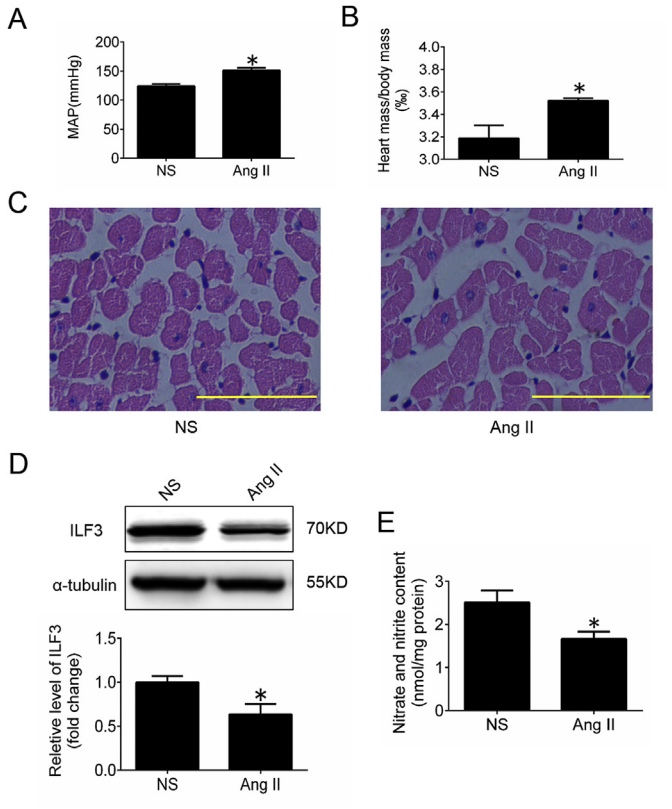

Fig. 1. ILF3 expression and NO production in hearts of cardiac hypertrophy model rats. A and B, The BP and ratio of heart mass to body mass in cardiac hypertrophy model rats. C, Representative images of heart sections stained with H&E (scale bar, 100 μm). D, Western blot analysis and quantification of ILF3 protein levels in the heart of cardiac hypertrophy model rats and controls. E, Total NO production in the left ventricular wall tissues of cardiac hypertrophy model rats and controls. Data were presented as mean ± SEM, n = 5/group, *P < 0.05 vs. NS. NS, saline; MAP, mean arterial pressure; H&E, hematoxylin and eosin.

3. Results

3.1. ILF3 expression and NO production were decreased significantly in cardiac hypertrophy model

To assess the rat model of cardiac hypertrophy, the BP (151.3 ± 4.5 vs. 124.2 ± 3.5 mmHg) (Fig. 1A), ratio of heart mass to body mass (3.521 ± 0.023 vs. 3.187 ± 0.117‰) (Fig. 1B), and cardiomyocyte size (Fig. 1C) were significantly increased in SD rats infused by Ang II for 4 weeks compared with saline infusion. To determine the potential role of ILF3 in the development of pathological cardiac hypertrophy, we observed a significant decrease of 36.45% in protein expression level of ILF3 in the cardiac hypertrophy model rat (Fig. 1D). Furthermore, the total NO production was significantly decreased in the left ventricle tissues of the Ang II-induced cardiac hypertrophy rat compared with the saline treated SD rats (Fig. 1E).

NRCMs were stimulated with differential concentrations of Ang II. It was found that the Ang II dose of 1–100 μM increased NRCM's size (Fig. 2A and B), along with an increase in the mRNA level of hypertrophic marker ANP and β-MHC after stimulation with Ang II (1 μM) for 48 h (Fig. 2C). In addition, the protein and mRNA level of ILF3 downregulation was confirmed in cultured NRCMs stimulated with Ang II (1 μM) for 48 h (Fig. 2D and E). The downregulation of ILF3 protein level caused by 1 μM Ang II in cultured NRCMs was most significant. Therefore, 1 μM Ang II was selected as the optimal dose in the following experiments (Fig. 2D). As indicated in Fig. 2F, Ang II significantly decreased total NO production (12.49 ± 0.33 vs. 15.46 ± 0.97 μmol/L)

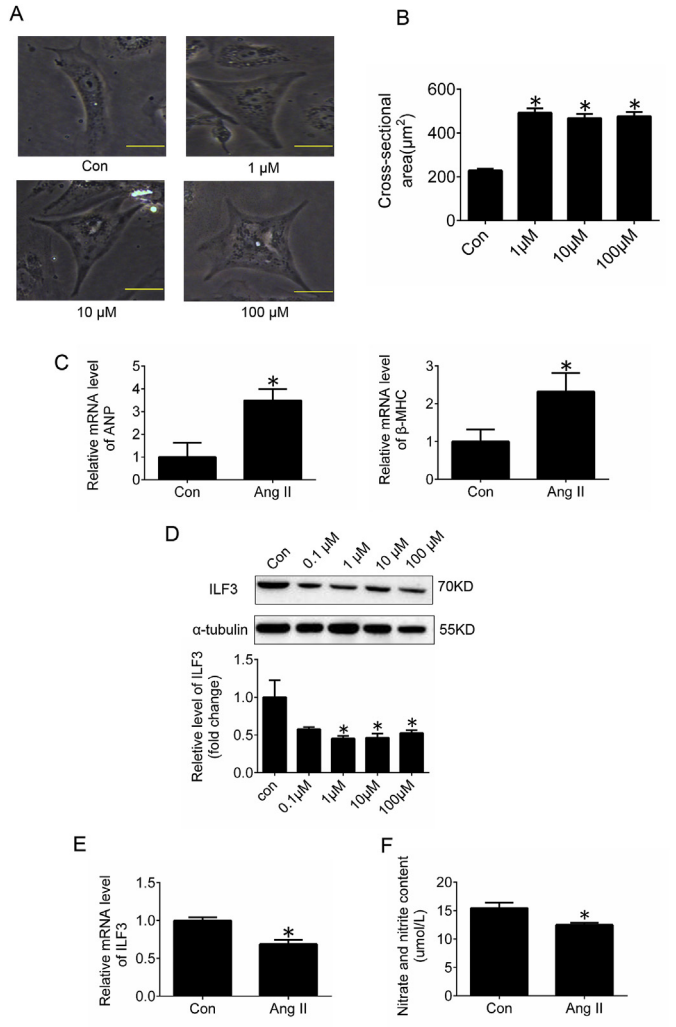

Fig. 2. ILF3 expression and NO production in hypertrophic NRCMs. A and B,Representative images and statistical graph of NRCMs size stimulated with different doses of Ang II or PBS for 48 h (scale bar, 10 μm). Quantification of cell cross-sectional area by measuring 100 random cells in each group. Data were presented as mean ± SEM, n = 100/group, *P < 0.05 vs. Con. C, Hypertrophic markers (ANP and β-MHC) mRNA levels in NRCM stimulated with Ang II (1 μM) or PBS. D, Western blot and quantification of ILF3 in NRCMs stimulated with different doses of Ang II or PBS. E, the level of ILF3 mRNA in NRCMs treated with Ang II or PBS. F, Total NO production in NRCMs treated with Ang II or PBS. Data were presented as mean ± SEM, n = 5/group, *P < 0.05 vs. Con. Con, control; PBS, phosphate-buffered saline; ANP, atrial natriuretic peptide; β-MHC, β-myosin heavy chain.

in cell culture medium of NRCMs compared with saline. Interestingly, as shown in Fig. 3, decrease in ILF3 expression (Fig. 3A) and NO production (Fig. 3B) in NRCMs treated with Ang II was significantly attenuated by Losartan (12.46 ± 0.34 vs. 15.16 ± 0.19 μmol/L).

3.2. ILF3 knockdown aggravated the deceased NO production in cardiac hypertrophy model

Specific ILF3 siRNA were transfected into NRCMs by using Lipofectamine 2000 to knock down ILF3. After FAM-labeled siRNA and Lipofectamine2000 were incubated with NRCMs for 6 h, green fluorescence was observed in the NRCMs, suggesting that ILF3 siRNA enters NRCMs *in vitro* (Fig. 4A). Moreover, the protein level of ILF3 was significantly decreased in the NRCMs treated with specific ILF3 siRNA compared with scramble siRNA controls (Fig. 4B). The cells were

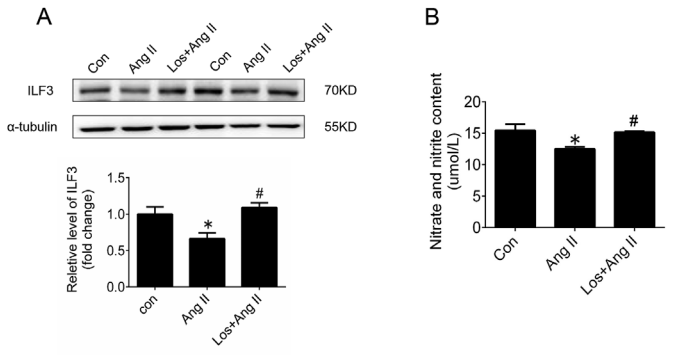

Fig. 3. The effects of Losartan on ILF3 expression and NO production in hypertrophic NRCMs. A, Representative protein bands and quantification of ILF3 protein levels in NRCMs stimulated with PBS, Ang II, or Ang II combined with Losartan. B, Total NO production in NRCMs stimulated with PBS, Ang II, or Ang II and Losartan together. Data were presented as mean ± SEM, n = 5/group, *P < 0.05 vs. Con; #P < 0.05 vs. Ang II. Con, control; PBS, phosphate-buffered saline.

subsequently treated with either Ang II or PBS for 48 h. Compared to the scramble siRNA control, ILF3 knockdown NRCMs remarkably aggravated the reduction of NO production (Fig. 4C) and NOS activity in the cardiac hypertrophy model induced by Ang II (Fig. 4D), as well as induced changes in NRCM's sizes (Fig. 4E and F). In addition, compared with scramble siRNA control, ILF3 knockdown NRCMs remarkably aggravated the accumulation of ADMA and the increase in the mRNA level of ANP in NRCMs treated with Ang II (Fig. 4G and H). These findings confirm that ILF3 also regulates the development of Ang II-triggered cardiomyocyte hypertrophy via modulating the NO production *in vitro*.

To further explore possible molecular mechanisms of ILF3 cardioprotective effects, DDAH1 mRNA and DDAH1 protein levels after ILF3 knockdown were detected in Ang II-treated cardiomyocyte. ILF3 knockdown induced a significant decrease in DDAH1 mRNA and protein levels, and remarkably aggravated the reduction of DDAH1 mRNA and protein levels in NRCMs treated with Ang II (Fig. 5A-B). The expressions of NOS isoforms were further detected, and it was found that the expression of nNOS was significantly increased in isolated cardiomyocyte treated with Ang II and ILF3 knockdown, while the expression of eNOS and iNOS were not affected by Ang II and ILF3 knockdown (Fig. 5C-E). These results suggest that the reduction in NO production by ILF3 knockdown may not be mediated by reducing the expression of NOS.

3.3. ILF3-mediated DDAH reduction caused ADMA accumulation and decrease in NO production in cardiac hypertrophy model rats

To further confirm the hypothesis that ILF3 exerts a cardio-protective function by reducing the accumulation of ADMA, we explored possible molecular mechanisms of cardiac hypertrophy in the rat model. FAM-labeled siRNAs were diluted in 5% glucose and mixed with *in vivo*-jet PEI, and directly injected intramyocardially on the left ventricular wall for 72 h. Green fluorescence was observed in the cardiomyocyte of the left ventricular wall, suggesting that ILF3 siRNA enter cardiomyocyte *in vivo* (Fig. 6A). Moreover, the protein level of ILF3 was significantly decreased in the left ventricular wall tissues treated with specific ILF3 siRNA, compared to scramble siRNA controls (Fig. 6B). Compared with the scramble siRNA control, ILF3 knockdown remarkably aggravated the reduction of total NO production and NOS activity (Fig. 6C and D), and further increased the level of ADMA in left ventricular wall tissues induced by Ang II (Fig. 6E). In order to explore the mechanism of NOS activity reduction, the expression of NOS isoforms was detected in the Ang II-induced cardiac hypertrophy model in adult rats. The expression of nNOS was also significantly increased in

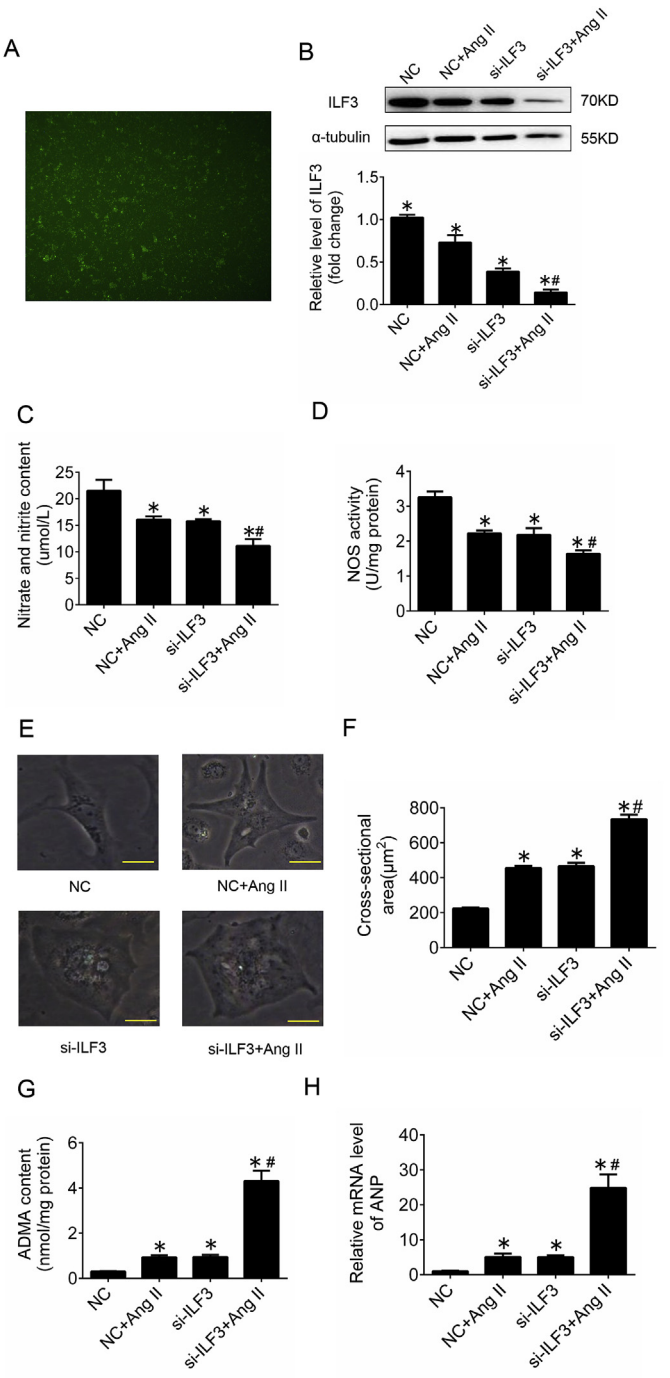

Fig. 4. Effect of ILF3 knockdown on decease in NO production caused by Ang II in NRCMs. A, Representative green fluorescence in NRCMs transfected with special FAM-labeled ILF3 siRNA using Lipofectamine 2000. B, Representative protein bands and quantification of ILF3 protein levels in NRCMs stimulated with PBS or Ang II combined with small interfering RNA. C, Total NO production in NRCMs stimulated with PBS or Ang II combined with small interfering RNA. D, NOS activity in NRCMs stimulated with PBS or Ang II combined with small interfering RNA. E and F, Representative images and statistical graph of NRCMs size stimulated with PBS or Ang II combined with siRNA (scale bar, 10 μm). Quantification of cell cross-sectional area by measuring 100 random cells in each group. Data were presented as mean ± SEM, n = 100/group, *P < 0.05 vs. NC; #P < 0.05 vs. Ang II + NC. G and F, The ADMA content and mRNA level of ANP in NRCMs stimulated with PBS or Ang II combined with small interfering RNA. Data were presented as mean ± SEM, n = 5/group, *P < 0.05 vs. NC; #P < 0.05 vs. Ang II + NC. NC, negative control (scramble sequence siRNA); siRNA, small interfering RNA.

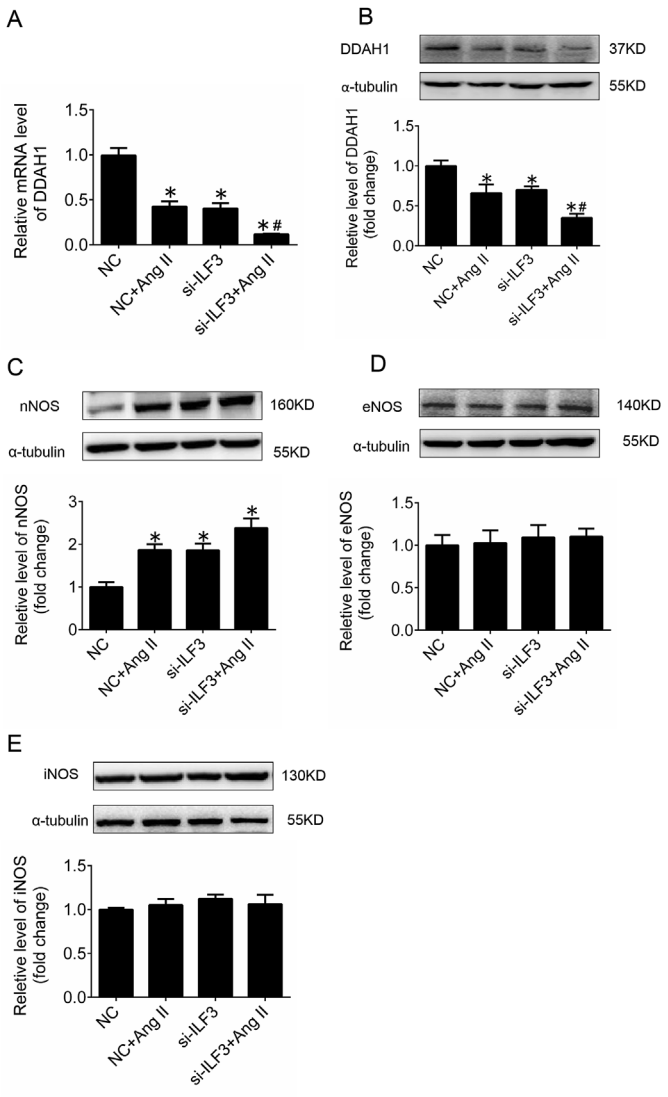

Fig. 5. Effect of ILF3 knockdown on changes in DDAH1 expression and NOS isoforms caused by Ang II in NRCMs. A and B, the mRNA and protein level of DDAH1 in NRCMs stimulated with PBS or Ang II combined with small interfering RNA. C-E, the representative protein bands and quantification of nNOS, eNOS, and iNOS protein levels in NRCMs stimulated with PBS or Ang II combined with siRNA. Data were presented as mean ± SEM, n = 5/group, *P < 0.05 vs. NC; #P < 0.05 vs. Ang II + NC. NC, negative control (scramble sequence siRNA); siRNA, small interfering RNA. eNOS, endothelial NOS; iNOS, inducible NOS; nNOS, neuronal NOS.

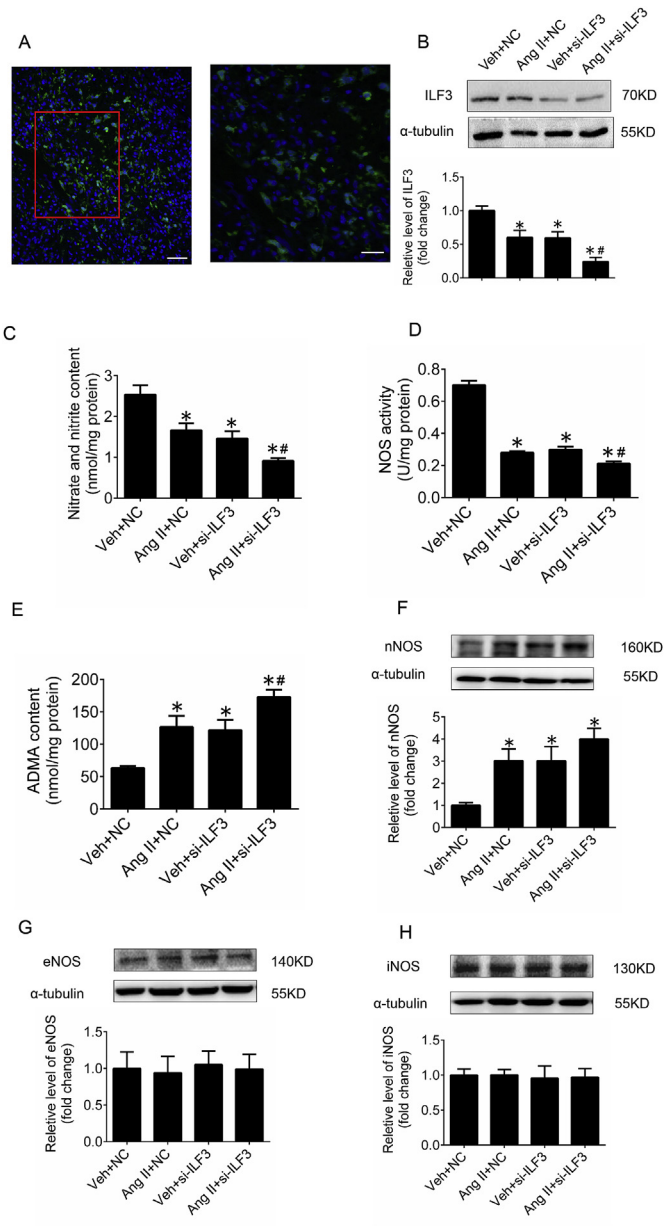

Fig. 6. Effects of ILF3 on ADMA accumulation and NO production in cardiac hypertrophy model rats. A, Representative green fluorescence in left ventricular wall tissues transfected with special FAM-labeled ILF3 siRNA through *in vivo*-jet PEI; the image on the left side was magnified by 200 times. The bar was 100 μm, the image on the right side was an enlarged view of the red box in the image on the left. The magnification was 400 times and the bar was 50 μm. B, Representative protein bands and quantification of ILF3 protein levels in left ventricular wall tissues of cardiac hypertrophy model rats and controls treated with siRNA. C-E, the total NO production, NOS activity, and ADMA content in left ventricular wall tissues of cardiac hypertrophy model rats and controls treated with siRNA. F–H, the representative protein bands and quantification of nNOS, eNOS, and iNOS protein levels in left ventricular wall tissues of cardiac hypertrophy model rats and controls treated with siRNA. Data were presented as mean ± SEM, n = 5/group, *P < 0.05 vs. Veh + NC; #P < 0.05 vs. Ang II + NC. Veh, vehicle; NC, negative control (scramble sequence siRNA); siRNA, small interfering RNA. eNOS, endothelial NOS; iNOS, inducible NOS; nNOS, neuronal NOS.

rats treated with Ang II and ILF3 knockdown, and the Ang II-induced increase in nNOS expression was not affected by ILF3 knockdown, while the expression of eNOS and iNOS was not affected by Ang II and ILF3 knockdown (Fig. 6F-H).

To explore the reasons for ADMA accumulation, DDAH1 protein expression was significantly decreased after intramyocardial injection of ILF3 siRNA. DDAH1 protein expression in other tissues such as kidney, liver, and brain, was not affected by ILF3 knockdown (Fig. 7A). It suggested that cardiac-specific DDAH1 decrease could be achieved by intramyocardial ILF3 siRNA injection. ILF3 knockdown induced a significant decrease in protein expression of DDAH1 (Fig. 7B) and mRNA level of DDAH1 (Fig. 7C). However, there was no significant difference in the expression of PRMT1 and DDAH2 after ILF3 knockdown (Fig. 7D and E). Moreover, DDAH activity in heart tissue was not affected by Ang II and ILF3 knockdown (Fig. 7F). These findings suggested that ILF3 regulates ADMA content by decreasing DDAH1 protein expression rather than affecting DDAH activity. Lastly, increase in the mRNA level of ANP in cardiac hypertrophic rats was significantly enhanced after ILF3 knockdown (Fig. 7G).

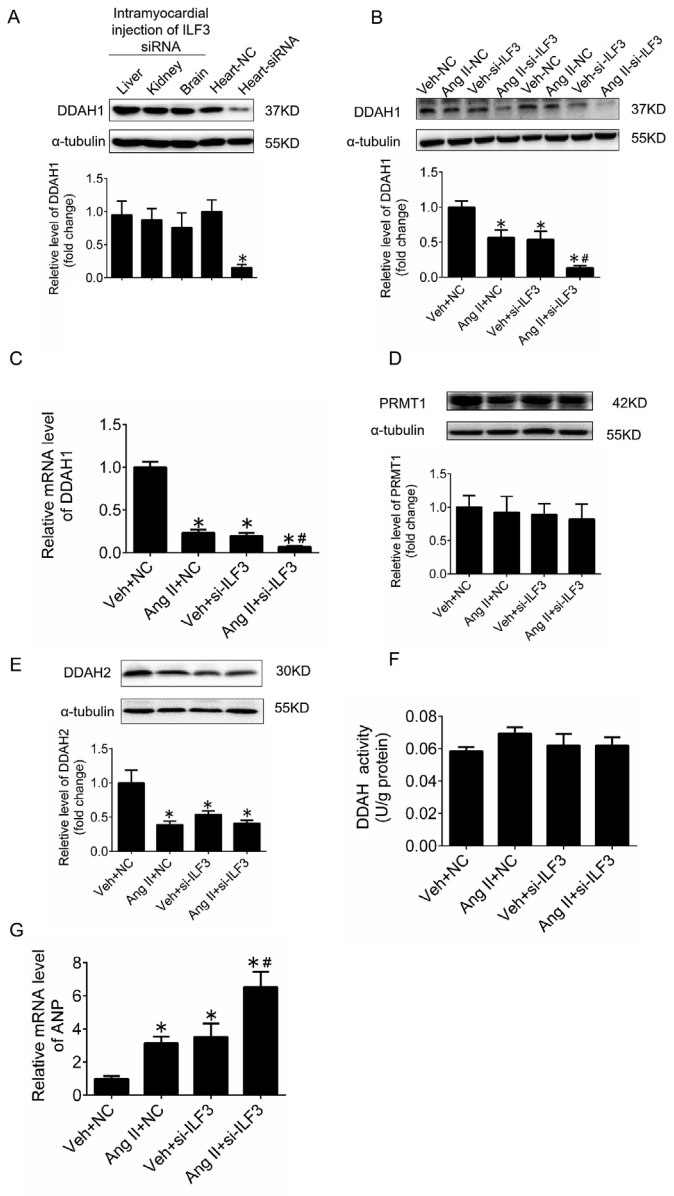

Fig. 7. Effects of ILF3 knockdown on DDAH1 expression reduction in cardiac hypertrophy model rats. A, Representative protein bands (top) and quantification histogram (bottom) for DDAH1 expression in different tissues after intramyocardial injection of ILF3 siRNA and in heart tissues after intramyocardial injection of NC. Data were presented as mean ± SEM, n = 5/group, *P < 0.05 vs. Heart-NC. B and C, the protein and mRNA levels of DDAH1 in left ventricular wall tissues of cardiac hypertrophy model rats and controls treated with siRNA. D and E, Protein expression of PRMT1 and DDAH2 in left ventricular wall tissues of cardiac hypertrophy model rats and controls treated with siRNA. F, DDAH activity in left ventricular wall tissues of cardiac hypertrophy model rats and controls treated with siRNA. G, Hypertrophic marker ANP mRNA levels in cardiac hypertrophy model rats and controls treated with siRNA. Data were presented as mean ± SEM, n = 5/group, *P < 0.05 vs. Veh + NC; #P < 0.05 vs. Ang II + NC. Veh, vehicle (saline); NC, negative control (scramble sequence siRNA); siRNA, small interfering RNA.

4. Discussion

The present study reveals the previously unrecognized biological function of ILF3 in cardiac hypertrophy. In our study, the major findings are that: 1) ILF3 plays a critical role in the pathogenesis of cardiac hypertrophy via reducing NO production; 2) The expression of ILF3 is regulated by Ang II in cardiac hypertrophy; and 3) In cardiac hypertrophy induced by Ang II, the increased ADMA content and decreased NO production is aggravated by ILF3 knockdown, which may be associated with downregulation of DDAH1. Based on the above findings, it is indicated that ILF3 is an important negative regulator of pathological cardiac hypertrophy via NO production.

Cardiac hypertrophy is a result of an adaptive growth response to neuro-hormonal activation and increased pressure loading, and if the overload factors persist, the cardiac hypertrophy will transform from an adaptive response to an organic lesion that eventually deteriorates into heart failure [34]. Overactivation of the renin-angiotensin system (increased Ang II) is an important mediating factor in the pathogenesis of cardiac hypertrophy [35]. Multiple cellular and molecular mechanisms have been determined to be involved in the pathogenesis of Ang II-induced cardiac hypertrophy, such as oxidative stress [36], monocyte infiltration [37], histone methyltransferase [38], etc. Among those, the reduction of NO production plays an important role in pathogenesis of cardiac hypertrophy, and NO produced by different NOS subtypes has different remodeling effects on cardiomyocytes. Our results showed that the expression of nNOS was significantly increased in isolated cardiomyocyte and rats treated with Ang II and ILF3 knockdown, and the expression of eNOS and iNOS was not affected by Ang II and ILF3 knockdown. The observed NOS subtypes expression changes in isolated cardiomyocyte were consistent with a previous study by Jang JH et al. [39]. However, NOS activity was reduced in cardiac hypertrophic cardiac cells and animal models, and NOS activity was further inhibited after ILF3 knockdown. In view of the complex role of NO produced by different NOS subtypes in the pathogenesis of cardiac hypertrophy [40,41]. In order to circumvent this problem, this study mainly explored the changes in the content of ADMA, an endogenous inhibitor of all NOS subtypes, thereby regulating the effect of NO production on myocardial cell remodeling.

The main function of ILF3 protein is to regulate the transcription and stability of mRNA, and promote the transfer of mRNAs bound to it from the nucleus to the cytoplasm, facilitating the translation process [18]. However, the role of ILF3 in cardiac hypertrophy has not yet been reported. To investigate the molecular mechanism by which ILF3 mediates its effects on cardiac hypertrophy, we first examined NO production, which plays a pivotal role in the development of cardiac hypertrophy [42]. We found that NO production was affected by ILF3 knockdown, and that ILF3 knockdown aggravated the decrease in total NO production in the cardiac hypertrophy model induced by Ang II, along with a significant increase in the mRNA level of ANP in cardiac hypertrophic rats after ILF3 knockdown. These findings suggested that anti-hypertrophic effects of ILF3 were associated with the increase in NO production.

In addition, we found that ADMA accumulation in cardiomyocyte of cardiac hypertrophy rat models, and ILF3 knockdown further increased its accumulation, indicating that ILF3 affects NO production by regulating the accumulation of ADMA. PRMT families, including enzymes that can methylate arginine residues on histones and other proteins, have been shown to be of importance in influencing various cellular functions [43]. In addition, type I PRMTs catalyze ADMA synthesis, and an increase in plasma ADMA levels is associated with endothelial dysfunction-related cardiovascular and pulmonary diseases [44,45]. In our previous study [29], it was confirmed that Ang II increased ADMA in the rostral ventrolateral medulla via upregulation of PRMT1 and downregulation of DDAH1, which inhibited the NOS activity and decreased total NO production, and resulted in a high level of sympathetic tone and BP. PRMT1, the predominant protein-arginine methyltransferase in cells, performs over 80% of PRMT activity in cells, and interacts with and is regulated by ILF3 [24,46]. In the present study, it was interesting that the protein level of PRMT1 was not affected by Ang II and ILF3 knockdown, which indicated that the anti-hypertrophic effect of ILF3 is independent of the protein expression of PRMT1. One detail issue that could not be ignored is the 50% reduction of the left ventricular DDAH1 protein expression increased cardiac ADMA ~2

fold. This detail suggests that ILF3 knockdown may also affect other factors that regulate cardiac ADMA content. Previously, others have shown there is an interaction between ILF3 and PRMT1 [23,24]. Although our findings showed that PRMT1 expression was not affected by ILF3 knockdown, ILF3 knockdown may affect PRMT1 activity. In addition, PRMT are a family of enzymes that can methylate arginine residues on histones and other proteins. Type I PRMT catalyzes the formation of ADMA, and type II catalyzes the formation of symmetric dimethylarginines (SDMA). PRMT1, 2, 3, 4, 6, and 8 display type I activity. Although PRMT1 is the predominant PRMT in mammalian cells, and performs over 80% of PRMT activity in the cells [47]. ILF3 knockdown may affect ADMA content by affecting other type I PRMTs such as PRMT3, other than PRMT1. Therefore, it is not difficult to understand that ILF3 knockdown results in a 2-fold increase in cardiac ADMA. Our results also showed that ILF3 knockdown reduced the expression of DDAH1 and increased the level of ADMA, and further reduced total NO production and NOS activity. Therefore, we speculate that ILF3 may affect DDAH1 in the cardiac hypertrophy model to regulate the accumulation of ADMA.

On the other hand, it has been reported that cardiomyocyte DDAH1 activity is dispensable for cardiac function under basal conditions, which attenuate cardiac hypertrophy and ventricular remodeling under stress conditions, possibly through regulation of ADMA and NO signaling [48]. Although there is no evidence showing the relationship between ILF3 and DDAH, our data showed that the expression levels of DDAH1 and DDAH2 in the Ang II-induced cardiac hypertrophy adult rats were decreased significantly. Furthermore, specific ILF3 knockdown further aggravated the decrease in DDAH1 expression. Previously published data show that the brain has 30–40 fold more DDAH1 protein than the heart, and also that the kidneys have 20–30 fold more DDAH1 than the heart [49]. Our results showed that there was no significant difference of DDAH1 expression between the heart, kidney, and the brain. While our data aimed to provide evidence that ILF3 knockdown decreased DDAH1 expression, since the above-mentioned effect of ILF3 knockdown was so dramatic, GeneTools had to prolonged exposure of the bands to show the minimal one, which is the band of heart-siRNA, so that the possible difference in expression of DDAH1 between other tissues and heart tissue was reduced, or resulted in no difference. In other words, prolonged exposure of protein bands did not affect our observation of the downregulation of DDAH1 expression following intramyocardial injection of ILF3 siRNA.

One of the main functions of ILF3 is stabilization of mRNA and facilitation of mRNA transport out of the nucleus. In this study, ILF3 knockdown induced a significant decrease in DDAH1 mRNA. These results suggest that ILF3 may play an important role in maintaining the stability of DDAH1 mRNA, so DDAH1 mRNA levels were also decreased after ILF3 knockdown. However, DDAH activity in heart tissue was not affected by Ang II and ILF3 knockdown. ADMA, as a substrate, is degraded to L-citrulline under the catalysis of DDAH. Our results showed that ADMA had a pathological accumulation in both Ang II treated and ILF3 knockdown cardiomyocyte. Assuming, the body will quickly compensate for the activity of DDAH in order to degrade the large amount of ADMA. It might be possible that at the time we analyzed DDAH activity, the body had already re-adjusted the function of DDAH to defend against the accumulation of ADMA. It is also possible that the DDAH activity is reduced at an earlier time point, most likely before ADMA accumulation. On the other hand, our findings showed that DDAH1 was down-regulated in Ang II treatment and ILF3 knockdown in cardiomyocytes. Taken together, the activity of DDAH in the cardiomyocytes was not affected. These results indicate that ILF3 can regulate the expression of DDAH1, thereby reducing the hydrolysis of ADMA, leading to the accumulation of ADMA. Further experiments are needed to confirm this hypothesis. In addition, considering that the previous interference with ILF3 siRNA can confirm the conclusion that ILF3 inhibits cardiac hypertrophy by ADMA-NO. We did not conduct further experiments on ILF3-overexpression, which may be a limitation in this study. Clearly, construction of ILF3 overexpressing adenovirus and observing its effects on DDHA1, NO, and cardiac hypertrophy can strengthen the evidence provided in this study.

To further explore the factors that regulate ILF3 expression in cardiac hypertrophy, our findings showed that ILF3 was significantly reduced in the Ang II-induced cardiac hypertrophy model, and this change was blocked by Losartan. These findings suggest that ILF3 expression regulated by Ang II was mediated by AT1R. Moreover, an abnormal increase in Ang II was associated with cardiac hypertrophy by regulating ILF3 expression.

In summary, this work determined the role of ILF3 in the pathogenesis of cardiac hypertrophy. It provided evidence that ILF3 protects against cardiac hypertrophy via modulation of NO production through protein regulation associated with ADMA metabolism. Collectively, it is indicated that ILF3 may serve as a new therapeutic target for inhibiting the development of cardiac hypertrophy.

Disclosures

No conflicts of interest.

Funding

This work was funded by the National Natural Science Foundation of China (No. 81800366, 81630012, and 81570385)

Acknowledgments

We sincerely acknowledge the support and help from the statistical professor Jian Lu (from the Department of Statistical Analysis, SMMU, China).

Appendix A. Supplementary data

Supplementary data to this article can be found online at https://doi.org/10.1016/j.niox.2019.09.002.

Abbreviations and acronyms

ADMA	asymmetric dimethylarginine
Ang II	angiotensin II
ANP	atrial natriuretic peptide
AT1R	angiotensin II type 1 receptor
β-MHC	β-myosin heavy chain
BP	blood pressure
DDAH1	dimethylarginine dimethylaminohydrolases 1
DDAH2	dimethylarginine dimethylaminohydrolases 2
eNOS	endothelial NOS
iNOS	inducible NOS
ILF3	interleukin enhancement binding factor 3
NO	nitric oxide
NOS	nitric oxide synthesis
nNOS	neuronal NOS
NRCMs	neonatal rat cardiomyocytes
PRMT1	protein arginine methyltransferases1
RVLM	rostral ventrolateral medulla
SD rats	Sprague Dawley rats

References

[1] R.A. Frieler, R.M. Mortensen, Immune cell and other noncardiomyocyte regulation of cardiac hypertrophy and remodeling, Circulation 131 (2015) 1019–1030.
[2] J. Tamargo, J. Lopez-Sendon, Novel therapeutic targets for the treatment of heart failure, Nat. Rev. Drug Discov. 10 (2011) 536–555.
[3] R.J. Everett, L. Tastet, M.A. Clavel, C.W.L. Chin, R. Capoulade, V.S. Vassiliou, J. Kwiecinski, M. Gomez, E.J.R. van Beek, A.C. White, S.K. Prasad, E. Larose, C. Tuck, S. Semple, D.E. Newby, P. Pibarot, M.R. Dweck, Progression of

hypertrophy and myocardial fibrosis in aortic stenosis: a multicenter cardiac magnetic resonance study, Circ Cardiovasc Imaging 11 (2018) 1–11.
[4] N. Koitabashi, D.A. Kass, Reverse remodeling in heart failure–mechanisms and therapeutic opportunities, Nat. Rev. Cardiol. 9 (2011) 147–157.
[5] J.H. van Berlo, M. Maillet, J.D. Molkentin, Signaling effectors underlying pathologic growth and remodeling of the heart, J. Clin. Investig. 123 (2013) 37–45.
[6] S. Matsushima, J. Kuroda, T. Ago, P. Zhai, J.Y. Park, L.H. Xie, B. Tian, J. Sadoshima, Increased oxidative stress in the nucleus caused by Nox4 mediates oxidation of HDAC4 and cardiac hypertrophy, Circ. Res. 112 (2013) 651–663.
[7] A. Lee, D. Jeong, S. Mitsuyama, J.G. Oh, L. Liang, Y. Ikeda, J. Sadoshima, R.J. Hajjar, C. Kho, The role of SUMO-1 in cardiac oxidative stress and hypertrophy, Antioxidants Redox Signal. 21 (2014) 1986–2001.
[8] K. Shibata, H. Shimokawa, N. Yanagihara, Y. Otsuji, M. Tsutsui, Nitric oxide synthases and heart failure - lessons from genetically manipulated mice, J. UOEH 35 (2013) 147–158.
[9] L.E. Dorn, L. Lasman, J. Chen, X. Xu, T.J. Hund, M. Medvedovic, J.H. Hanna, J.H. van Berlo, F. Accornero, The m(6)A mRNA methylase METTL3 controls cardiac homeostasis and hypertrophy, Circulation (2018) 533–545.
[10] L. Song, L. Wang, F. Li, A. Yukht, M. Qin, H. Ruther, M. Yang, A. Chaux, P.K. Shah, B.G. Sharifi, Bone marrow-derived tenascin-C attenuates cardiac hypertrophy by controlling inflammation, J. Am. Coll. Cardiol. 70 (2017) 1601–1615.
[11] G. Voros, J. Ector, C. Garweg, W. Droogne, J. Van Cleemput, N. Peersman, P. Vermeersch, S. Janssens, Increased cardiac uptake of ketone bodies and free fatty acids in human heart failure and hypertrophic left ventricular remodeling, Circ Heart Fail 11 (2018) e004953.
[12] M.V. Brahmajothi, D.L. Campbell, Heterogeneous basal expression of nitric oxide synthase and superoxide dismutase isoforms in mammalian heart : implications for mechanisms governing indirect and direct nitric oxide-related effects, Circ. Res. 85 (1999) 575–587.
[13] Y. Lin, L.N. Wang, Y.H. Xi, H.Z. Li, F.G. Xiao, Y.J. Zhao, Y. Tian, B.F. Yang, C.Q. Xu, L-arginine inhibits isoproterenol-induced cardiac hypertrophy through nitric oxide and polyamine pathways, Basic Clin. Pharmacol. Toxicol. 103 (2008) 124–130.
[14] M. Ozaki, S. Kawashima, T. Yamashita, T. Hirase, Y. Ohashi, N. Inoue, K. Hirata, M. Yokoyama, Overexpression of endothelial nitric oxide synthase attenuates cardiac hypertrophy induced by chronic isoproterenol infusion, Circ. J. 66 (2002) 851–856.
[15] J. Ren, L. Yang, W. Tian, M. Zhu, J. Liu, P. Lu, J. Li, L. Yang, Z. Qi, Nitric oxide synthase inhibition abolishes exercise-mediated protection against isoproterenol-induced cardiac hypertrophy in female mice, Cardiology 130 (2015) 175–184.
[16] E. Cavusoglu, C. Ruwende, V. Chopra, S. Yanamadala, C. Eng, D.J. Pinsky, J.D. Marmur, Relationship of baseline plasma ADMA levels to cardiovascular outcomes at 2 years in men with acute coronary syndrome referred for coronary angiography, Coron. Artery Dis. 20 (2009) 112–117.
[17] C. Zoccali, F. Mallamaci, R. Maas, F.A. Benedetto, G. Tripepi, L.S. Malatino, A. Cataliotti, I. Bellanuova, R. Boger, C. Investigators, Left ventricular hypertrophy, cardiac remodeling and asymmetric dimethylarginine (ADMA) in hemodialysis patients, Kidney Int. 62 (2002) 339–345.
[18] S. Castella, R. Bernard, M. Corno, A. Fradin, J.C. Larcher, Ilf3 and NF90 functions in RNA biology, Wiley Interdiscip Rev RNA 6 (2015) 243–256.
[19] A.M. Parrott, M.B. Mathews, Novel rapidly evolving hominid RNAs bind nuclear factor 90 and display tissue-restricted distribution, Nucleic Acids Res. 35 (2007) 6249–6258.
[20] J.C. Larcher, L. Gasmi, W. Viranaicken, B. Edde, R. Bernard, I. Ginzburg, P. Denoulet, Ilf3 and NF90 associate with the axonal targeting element of Tau mRNA, FASEB J. 18 (2004) 1761–1763.
[21] Y. Yamada, T. Nishida, S. Ichihara, M. Sawabe, N. Fuku, Y. Nishigaki, Y. Aoyagi, M. Tanaka, Y. Fujiwara, H. Yoshida, S. Shinkai, K. Satoh, K. Kato, T. Fujimaki, K. Yokoi, M. Oguri, T. Yoshida, S. Watanabe, Y. Nozawa, A. Hasegawa, T. Kojima, B.G. Han, Y. Ahn, M. Lee, D.J. Shin, J.H. Lee, Y. Jang, Association of a polymorphism of BTN2A1 with myocardial infarction in East Asian populations, Atherosclerosis 215 (2011) 145–152.
[22] C.N. Vrakas, A.B. Herman, M. Ray, S.E. Kelemen, R. Scalia, M.V. Autieri, RNA stability protein ILF3 mediates cytokine-induced angiogenesis, FASEB J. (2018) 3304–3316.
[23] Z. Nemeth, A. Cziraki, S. Szabados, B. Biri, S. Keki, A. Koller, Elevated levels of asymmetric dimethylarginine (ADMA) in the pericardial fluid of cardiac patients correlate with cardiac hypertrophy, PLoS One 10 (2015) e0135498.
[24] J. Tang, P.N. Kao, H.R. Herschman, Protein-arginine methyltransferase I, the predominant protein-arginine methyltransferase in cells, interacts with and is regulated by interleukin enhancer-binding factor 3, J. Biol. Chem. 275 (2000) 19866–19876.
[25] S. Gathiaka, B. Boykin, T. Caceres, J.M. Hevel, O. Acevedo, Understanding protein arginine methyltransferase 1 (PRMT1) product specificity from molecular dynamics, Bioorg. Med. Chem. 24 (2016) 4949–4960.
[26] Q. Zhou, S.S. Wei, H. Wang, Q. Wang, W. Li, G. Li, J.W. Hou, X.M. Chen, J. Chen, W.P. Xu, Y.G. Li, Y.P. Wang, Crucial role of ROCK2-mediated phosphorylation and upregulation of FHOD3 in the pathogenesis of angiotensin II-induced cardiac hypertrophy, Hypertension 69 (2017) 1070–1083.
[27] X. Tan, P.L. Jiao, Y.K. Wang, Z.T. Wu, X.R. Zeng, M.L. Li, W.Z. Wang, The phosphoinositide-3 kinase signaling is involved in neuroinflammation in hypertensive rats, CNS Neurosci. Ther. 23 (2017) 350–359.
[28] Y.K. Wang, Q. Yu, X. Tan, Z.T. Wu, R.W. Zhang, Y.H. Yang, W.J. Yuan, Q.K. Hu, W.Z. Wang, Centrally acting drug moxonidine decreases reactive oxygen species via inactivation of the phosphoinositide-3 kinase signaling in the rostral ventrolateral medulla in hypertensive rats, J. Hypertens. 34 (2016) 993–1004.
[29] X. Tan, J.K. Li, J.C. Sun, P.L. Jiao, Y.K. Wang, Z.T. Wu, B. Liu, W.Z. Wang, The asymmetric dimethylarginine-mediated inhibition of nitric oxide in the rostral ventrolateral medulla contributes to regulation of blood pressure in hypertensive rats, Nitric Oxide 67 (2017) 58–67.
[30] D. Chen, K.Q. Zhang, B. Li, D.Q. Sun, H. Zhang, Q. Fu, Epigallocatechin-3-gallate ameliorates erectile function in aged rats via regulation of PRMT1/DDAH/ADMA/NOS metabolism pathway, Asian J. Androl. 19 (2017) 291–297.
[31] C.J. Yu, L.L. Tang, C. Liang, X. Chen, S.Y. Song, X.Q. Ding, K.Y. Zhang, B.L. Song, D. Zhao, X.Y. Zhu, H.L. Li, Z.R. Zhang, Angiotensin-Converting enzyme 3 (ACE3) protects against pressure overload-induced cardiac hypertrophy, J Am Heart Assoc 5 (2016) 1–15.
[32] X. Chen, S. Zhao, Y. Xia, Z. Xiong, Y. Li, L. Tao, F. Zhang, X. Wang, G protein coupled receptor kinase-2 upregulation causes kappa-opioid receptor desensitization in diabetic heart, Biochem. Biophys. Res. Commun. 482 (2017) 658–664.
[33] B.L. Chen, Y.D. Ma, R.S. Meng, Z.J. Xiong, H.N. Wang, J.Y. Zeng, C. Liu, Y.G. Dong, Activation of AMPK inhibits cardiomyocyte hypertrophy by modulating of the FOXO1/MuRF1 signaling pathway in vitro, Acta Pharmacol. Sin. 31 (2010) 798–804.
[34] L. Neyses, T. Pelzer, The biological cascade leading to cardiac hypertrophy, Eur. Heart J. 16 (Suppl N) (1995) 8–11.
[35] Y.X. Luo, X. Tang, X.Z. An, X.M. Xie, X.F. Chen, X. Zhao, D.L. Hao, H.Z. Chen, D.P. Liu, SIRT4 accelerates Ang II-induced pathological cardiac hypertrophy by inhibiting manganese superoxide dismutase activity, Eur. Heart J. 38 (2017) 1389–1398.
[36] D.F. Dai, S.C. Johnson, J.J. Villarin, M.T. Chin, M. Nieves-Cintron, T. Chen, D.J. Marcinek, G.W. Dorn 2nd, Y.J. Kang, T.A. Prolla, L.F. Santana, P.S. Rabinovitch, Mitochondrial oxidative stress mediates angiotensin II-induced cardiac hypertrophy and Galphaq overexpression-induced heart failure, Circ. Res. 108 (2011) 837–846.
[37] L. Wang, Y.L. Zhang, Q.Y. Lin, Y. Liu, X.M. Guan, X.L. Ma, H.J. Cao, Y. Liu, J. Bai, Y.L. Xia, J. Du, H.H. Li, CXCL1-CXCR2 axis mediates angiotensin II-induced cardiac hypertrophy and remodelling through regulation of monocyte infiltration, Eur. Heart J. 39 (2018) 1818–1831.
[38] L. Yu, G. Yang, X. Weng, P. Liang, L. Li, J. Li, Z. Fan, W. Tian, X. Wu, H. Xu, M. Fang, Y. Ji, Y. Li, Q. Chen, Y. Xu, Histone methyltransferase SET1 mediates angiotensin II-induced endothelin-1 transcription and cardiac hypertrophy in mice, Arterioscler. Thromb. Vasc. Biol. 35 (2015) 1207–1217.
[39] J.H. Jang, J.N. Chun, S. Godo, G. Wu, H. Shimokawa, C.Z. Jin, J.H. Jeon, S.J. Kim, Z.H. Jin, Y.H. Zhang, ROS and endothelial nitric oxide synthase (eNOS)-dependent trafficking of angiotensin II type 2 receptor begets neuronal NOS in cardiac myocytes, Basic Res. Cardiol. 110 (2015) 21.
[40] T. Kempf, K.C. Wollert, Nitric oxide and the enigma of cardiac hypertrophy, Bioessays 26 (2004) 608–615.
[41] S. Inaba, M. Iwai, M. Furuno, H. Kanno, I. Senba, H. Okayama, M. Mogi, J. Higaki, M. Horiuchi, Role of angiotensin-converting enzyme 2 in cardiac hypertrophy induced by nitric oxide synthase inhibition, J. Hypertens. 29 (2011) 2236–2245.
[42] A.L. Moens, E. Takimoto, C.G. Tocchetti, K. Chakir, D. Bedja, G. Cormaci, E.A. Ketner, M. Majmudar, K. Gabrielson, M.K. Halushka, J.B. Mitchell, S. Biswal, K.M. Channon, M.S. Wolin, N.J. Alp, N. Paolocci, H.C. Champion, D.A. Kass, Reversal of cardiac hypertrophy and fibrosis from pressure overload by tetrahydrobiopterin: efficacy of recoupling nitric oxide synthase as a therapeutic strategy, Circulation 117 (2008) 2626–2636.
[43] H. Wei, R. Mundade, K.C. Lange, T. Lu, Protein arginine methylation of non-histone proteins and its role in diseases, Cell Cycle 13 (2014) 32–41.
[44] X. Liu, X. Xu, R. Shang, Y. Chen, Asymmetric dimethylarginine (ADMA) as an important risk factor for the increased cardiovascular diseases and heart failure in chronic kidney disease, Nitric Oxide 78 (2018) 113–120.
[45] K. Krzyzanowska, F. Mittermayer, M. Wolzt, G. Schernthaner, ADMA, cardiovascular disease and diabetes, Diabetes Res. Clin. Pract. 82 (Suppl 2) (2008) S122–S126.
[46] M. Ohno, J. Komakine, E. Suzuki, M. Nishizuka, S. Osada, M. Imagawa, Interleukin enhancer-binding factor 3 functions as a liver receptor homologue-1 co-activator in synergy with the nuclear receptor co-activators PRMT1 and PGC-1alpha, Biochem. J. 437 (2011) 531–540.
[47] H. Wei, R. Mundade, K.C. Lange, T. Lu, Protein arginine methylation of non-histone proteins and its role in diseases, Cell Cycle 13 (2014) 32–41.
[48] X. Xu, P. Zhang, D. Kwak, J. Fassett, W. Yue, D. Atzler, X. Hu, X. Liu, H. Wang, Z. Lu, H. Guo, E. Schwedhelm, R.H. Boger, P. Chen, Y. Chen, Cardiomyocyte dimethylarginine dimethylaminohydrolase-1 (DDAH1) plays an important role in attenuating ventricular hypertrophy and dysfunction, Basic Res. Cardiol. 112 (2017) 1–11.
[49] X. Liu, X. Xu, R. Shang, Y. Chen, Asymmetric dimethylarginine (ADMA) as an important risk factor for the increased cardiovascular diseases and heart failure in chronic kidney disease, Nitric Oxide 78 (2018) 113–120.